Review

Israel Journal of Chemistry

DOI: 10.1002/ijch.201000014

Electrochemistry of Single Nanoparticles via Electrocatalytic Amplification

Allen J. Bard,*[a] Hongjun Zhou,[a] and Seong Jung Kwon[a]

Abstract: Recent experiments on the observation of collisions of single nanoparticles (NPs) with an electrode through amplification of the current by electrocatalysis are described. Systems in which the particles adhere to the electrode upon collision produce a step and staircase response, while those in which particles only interact for a short time with the electrode produce a spike or blip, with little change in the steady state current. Examples of both behaviors, e.g., Pt NPs on a Au electrode for hydrazine oxidation (staircase response) and IrO_x NPs on a Pt electrode for water oxidation (blip response) are shown. Controlling the nature of the electrode surface is important in generating useful responses, for example, in the case of gold NPs on an oxidized Pt electrode for borohydride oxidation.

Keywords: electrocatalytic amplification · electrochemistry · nanoparticles · single-molecule studies

1. Introduction

I'm honored to have this special issue dedicated to the 2008 Wolf Prize in Chemistry, and I thought it would be appropriate to submit a paper on a topic related to the work mentioned for that award, i.e., single molecule detection. The possibility of observing and studying single molecules or individual nm-size particles is a rather recent one (barely 20 years old),[1,2] but one of immense importance. The bulk of the work has been carried out with spectroscopy (especially via fluorescence) and by scanning probe microscopy, almost always with molecules that are immobilized at an interface. We have been working on electrochemical, or spectroelectrochemical, approaches in this field. In all examples, detection depends upon obtaining very large amplification factors, where the single molecule produces a large number of detectable events (e.g., photon emission, electron transfers, catalytic products). In spectroscopy, this is provided by the fluorescence that can be observed by bombarding the particle with a large photon flux (often with attendant problems with photochemical stability of the molecule under observation). A spectroelectrochemical approach, combining fluorescent detection with electrochemical processes to observe changes upon electron transfer, has been demonstrated.[3,4] This approach is limited by the need to study molecules that have both the spectroscopic and electrochemical properties required, which leads to a rather restricted palette of useful candidate molecules.

An alternative approach, which is the subject of this paper, involves molecular detection purely by electrochemical means. For example, as shown in earlier studies, the needed high amplification can be obtained by repeated redox turnover of a single molecule trapped between two electrodes.[5,6,7] Since the initial report of this approach, related studies have been reported, where the molecule is trapped between an ultramicroelectrode (UME) and a mercury pool.[8] A different method of amplification, as we describe in this review, involves detection of nm-size electrocatalytic particles as they collide with an inert electrode (i.e., one that does not carry out the electrochemical reaction of interest at an appreciable rate).

The reason one is interested in single molecule electrochemistry (as with analogous spectroscopic studies) is the desire to learn about behavior and processes that cannot be discovered from studies of large ensembles of molecules as traditionally carried out. The treatments of electrode processes, for example, do not really address the extreme complexity of what is occurring on a molecular basis and are almost always based on differential equations, such as the diffusion equation, that hold for large numbers of molecules and the average behavior of individual molecules. The same is true when we consider the kinetics of the electron transfer reaction at an electrode in terms of an averaged rate constant. Consider a molecular picture of an electrode reaction. Think of a molecule in the bulk solution about 5 μm from the electrode, which undergoes a random walk to eventually end up at the

[a] A. J. Bard, H. Zhou, S. J. Kwon
Center for Electrochemistry, Department of Chemistry and Biochemistry,
The University of Texas at Austin, Austin, TX 78712, USA
phone: +1 512 471-3761
fax: +1 512 471-0088
e-mail: ajbard@mail.utexas.edu

Allen J. Bard was born in New York City in 1933 and attended public schools there, including the Bronx High School of Science (1948-51). He attended The City College of the College of New York (CCNY) (B.S., 1955) and Harvard University (M.A., 1956, Ph.D., 1958). Dr. Bard joined the faculty at The University of Texas at Austin (UT) in 1958, and has spent his entire career there, holding the Hackerman-Welch Regents Chair in Chemistry since 1985. Sabbaticals and guest lectures have taken him to Paris, the California Institute of Technology, Cornell University, and back to Harvard. He has worked as mentor and collaborator with 80 Ph.D students, 17 M.S. students, 150 postdoctoral associates, and numerous visiting scientists. Bard's publications include over 800 peer-reviewed research papers, 75 book chapters, and three books, as well as serving as Editor-in-Chief of the Journal of the American Chemical Society 1982–2001. In 2008, he was awarded the Wolf Foundation Prize in Chemistry, jointly with William E. Moerner of Stanford University, "for the ingenious creation of a new field of science, single molecule spectroscopy and electrochemistry, with impact at the nanoscopic regime, from the molecular and cellular domain to complex material systems." His research interests involve the application of electrochemical methods to the study of chemical problems and include investigations in scanning electrochemical microscopy, electrogenerated chemiluminescence and photoelectrochemistry.

Hongjun Zhou received his B.S. and M.S. in Polymer Science and Engineering from Nanjing University (China) in 2000 and 2003, respectively. He then obtained his Ph.D. from the State University of New York at Stony Brook in 2009. He is currently working as a post-doc fellow in the group of Professor Allen J. Bard at the University of Texas at Austin. His research interests include nanoparticle synthesis, and characterization and electrochemistry of single nanoparticle collisions.

Seong Jung Kwon was born in Daegu, South Korea, in 1980. He received a Bachelor's degree in 2002 from Korea Advanced Institute of Science and Technology (KAIST). After that, he continued his research there in the group of Prof. Juhyoun Kwak at the Department of Chemistry. In 2008 he received a Ph.D. degree, working on the electrochemically signal-amplified immunosensor. He remained in the same group as a postdoctoral fellow until Aug. 2009. In Sept. 2009 he joined the group of Prof. Allen J. Bard at the University of Texas at Austin as a postdoctoral fellow. His research interests include electrochemical detection of biomolecules and investigation of single nanoparticle behavior.

"electrode surface," i.e., close enough to the electrode that an electron transfer is highly probable. For a diffusion coefficient, D, of 10^{-5} cm^2/s, on average this would take about 12 ms. However some molecules at this position would reach the electrode more quickly, and others might diffuse in the opposite direction and take a much longer time. In a sense, this is a remarkably short time, given that the molecule, say 0.5 nm in size, has to move a distance that is 10^4 times its size (equivalent to a 2-m-tall person moving to cover a distance of 20 km). Once in the vicinity of the electrode, the molecule spends a sufficiently long time to sample many environments and eventually, perhaps through many rapid multiple collisions, undergoes an electron transfer reaction.[9] The actual molecular nature of the electron transfer step (e.g., the distance of the molecule from the actual metal/solvent interface, the orientation and configuration of the molecule) and the number of collisions needed before an electron transfer occurs is not known.

While nanoparticles (NPs) are not the same as molecules, a major trend in chemistry over the last decades (i.e., in supramolecular chemistry and nanostructures) is to show that in many ways these larger (quasi-bulk material) structures behave as "super molecules" and can be described in terms of molecular orbitals (just as molecules can be described in terms of atomic orbitals). They have the advantage that the response seen with NPs is often much larger than that of molecules, as seen in this work, although it is much more difficult to prepare identical entities and characterize them. Perhaps, as the described techniques develop, one will be able to work with smaller and smaller NPs with more uniform composition and structure, and eventually carry out the same kinds of studies with smaller molecules.

When a single metal NP contacts an electrode, the NP will become charged. However, only a few electrons will transfer, and the current will be too small to be distinguished from the background level or noise. However, if the NP can electrocatalyze some reaction that the contacting electrode cannot ($O + n_oe \rightarrow R$, e.g., where O is H^+ and R is H_2), the current can be much higher because of the continued electron flow involved with this reaction. This provides the needed amplification for single particle detection. The observed response depends on how long the NP remains on the electrode surface. If the NP sticks to the electrode surface, the steady state diffusion-controlled current at the NP (assuming spherical diffusion and a very fast electrocatalytic reaction) is

$$i_{ss} = 4\pi(ln2)n_0FD_0C_0r_0 \quad (1)$$

where n_0 is the number of electrons transferred, F is the Faraday, D_0 is diffusion coefficient of O, C_0 is the concentration of O, and r_0 is the radius of the NP.[10] In this situation, the current from each new NP contact adds to the

previous one and a "staircase" response is observed.

However, if the NP doesn't stick to the electrode, the total charge transferred is determined by NP size, its residence time, the rate of the electrocatalytic reaction, and the rate of charge transfer from the electrode, in a more complex way. In this situation, each NP contact results in a transient current or "blip" superimposed on a constant background current. Both types of responses have been observed and are described in the following sections.

2. Metal NPs (Sticking and Staircase Response)

2.1. Pt NPs/C UME /Proton Reduction[11]

As shown in Figure 1a, proton reduction is sluggish at a carbon electrode in 50 mM sodium dihydrogen citrate at potentials (E) positive of –0.5 V (vs. NHE). However if the C electrode is covered with Pt NPs (or at a pure Pt electrode), a steady-state diffusion-limited current (i_{ss}) is seen at $E < -0.3$ V.[12] Here, i_{ss} for a single Pt NP sticking on the electrode surface can be estimated by Equation 1. This current is ~ 60 pA for a spherical particle of 4 nm diameter. Figure 1b shows the current transient at a carbon fiber electrode in a solution before and after injection of Pt NPs. The Pt NPs were made by $NaBH_4$ reduction of H_2PtCl_6 in the presence of sodium citrate and the sizes ranged from 2 to 6 nm (average 4 ± 0.8 nm).[13] The expected current profile is a transient with a rapid decay to a steady state level. Different types of responses were shown in Figure 1c. The characteristics of an individual current time (i-t) profile are determined by many factors, including NP size, residence time, and the interaction between the NP and the electrode. The current decays over a period of tens of seconds, which may be caused by deactivation of the particle surface, either from adsorption of an impurity from solution or by blockage from the hydrogen produced.[14] The amplitude of the currents is about 40–80 pA (Figure 1d), which is consistent with the sizes of Pt NPs injected, as determined by TEM.

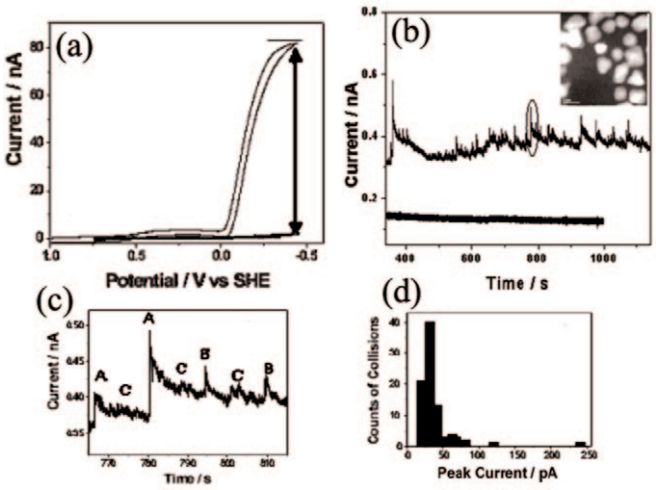

Figure 1. (a) Electrochemical reduction of proton at carbon fiber electrode without (bottom curve) and with (upper curve) Pt nanoparticles on the surface in air-saturated, 50 mM sodium dihydrogen citrate solution (fiber diameter, 8 μm; scan rate, 100 mV/s). (b) Current transient at a C fiber electrode in 50 mM sodium dihydrogen citrate solution in the absence (bottom curve) and presence (upper curve) of Pt citrate NPs. Particle concentration is about 25 pM. Inset is a TEM image of representative Pt NPs. (c) Zoom-in of panel (b) showing three kinds of collisions distinguished by the current amplitude and frequency. (d) Statistics of number of collisions versus their peak currents. Collisions with peak currents less than 15 pA, are not included in this figure. Inset is a TEM image of representative Pt nanoparticles.

When the potential of the electrode was shifted positive, the amplitude of spikes decreased, which is in agreement with Figure 1a. As expected from Equation 1, the proton concentration affects the amplitude of spikes. However, if $[H^+]$ was increased further to increase the size of the response, the Pt NPs became unstable because of protonation of the carboxylate groups of the stabilizing citrate. In this case (Figure 2a), very large spikes were seen after injection of particles, eventually disappearing (after ~600 s for this case) as the NPs grew and precipitated.

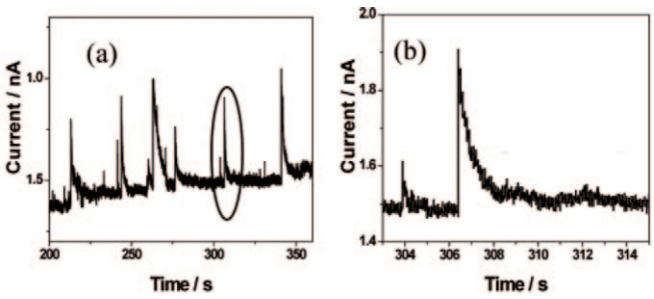

Figure 2. (a) Current transient at a carbon fiber electrode in 10 mM perchloric acid and 20 mM sodium perchlorate in the presence of Pt citrate NPs. Particle concentration is about 12.5 pM. (b) Zoom in of panel (a).

2.2. Pt NPs/Thiol-Modified Au Electrode/(H_2O_2 Reduction)[11]

A Au UME was modified with benzenedimethanethiol to decrease the background current and increase the interaction between NPs and the electrode. A self-assembled monolayer (SAM) of thiol thus formed was capable of electron tunneling to solution species.[15] In the presence of thiol groups on the electrode, Pt particles were expected to bind strongly with the electrode. Discrete steps (Figure 3a) and a staircase response were observed after injection of Pt citrate NPs into a 50 mM H_2O_2 solution. In addition to the steps, small current fluctuations were also recorded (Figure 3b). These fluctuations are analogous to collisions as shown in Figure 1c, and may be caused by smaller Pt particles in the preparation.

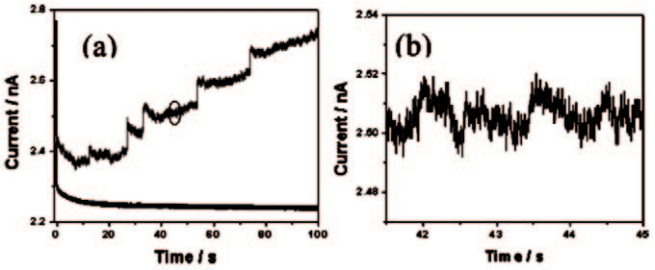

Figure 3. (a) Current transient at a benzenedimethanethiol-modified 25 μm diameter Au electrode at 0.1 V (vs. SHE) in 0.1 M PBS pH 7.4 buffer solution containing 50 mM hydrogen peroxide in the absence (bottom curve) and presence (upper curve) of 25 pM Pt NPs. The background current was increased by 1.5 nA for clarity. (b) Zoom-in of panel (a).

2.3. Pt NPs/ C, Au Electrodes/Hydrazine Oxidation[16,17]

Hydrazine oxidation shows distinguishable oxidation behavior with Pt, Au, and C electrodes. For example, the onset oxidation potential of hydrazine oxidation on a Pt UME is more negative than that on a Au UME (Figure 4a). This gives a potential window in which the reaction rate at Pt is significantly larger than that at Au.

Figure 4b shows a typical current–time curve recorded at the Au UME after injection of Pt NPs (citrate stabilized, average ~3.6 nm), where the current increased in a stepwise fashion. Most of the steps were in the range of 40–65 pA, which agrees well with 55 pA estimated from steady state current for 3.6-nm-sized Pt NPs. Some smaller current steps (Figure 4c) were also observed. In each current step, the current increased very rapidly (rise-time was about 40–100 μs) and then remained at a steady value.

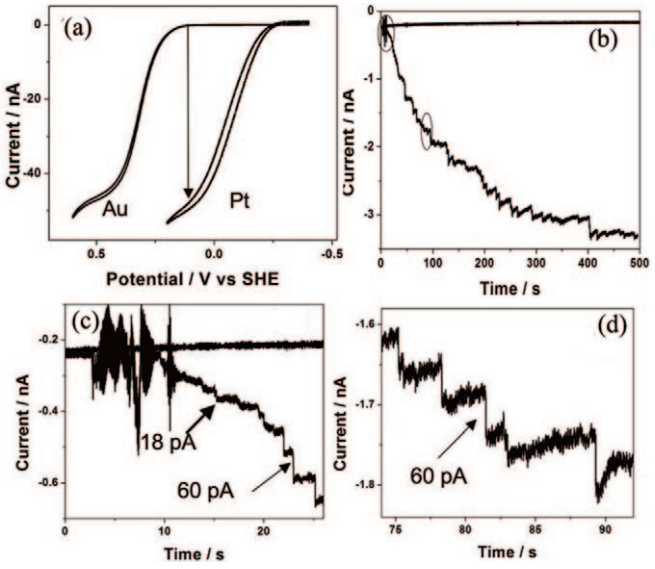

Figure 4. (a) Hydrazine oxidation at Au and Pt UMEs. Scan rate, 50 mV/s. (b) Current transient recorded at Au UME before and after Pt NP solution was injected. (c) Zoom-in of the initial part of panel (b), and (d) zoom-in of the intermediate part of panel (b), as marked. Colloidal solution: ~36 pM Pt NP solution; particle size, ~3.6 nm; electrode diameter, 10 μm; electrolyte, 10 mM hydrazine, 50 mM PBS buffer, pH ~7.5.

Since each current step signals a single particle collision event, the size distribution of NPs is reflected by the distribution of current steps. Figures 5b and 5d show a comparison of the distribution of the current steps and particle sizes. The occasional larger peak currents are probably caused by collisions of nanoparticle aggregates.

Different experimental conditions were also investigated to test the proposed collision model. When the hydrazine concentration was changed, the amplitude of the current step changed proportionally. When the concentration of Pt NPs was increased, the peak frequency was increased while the current amplitudes emained the same. Injection of larger Pt NPs resulted in bigger current steps. When a larger Au UME (25 μm) was used instead of a 10 μm Au UME, the collision frequency increased about twice.

To study factors influencing the probability of a NP sticking, experiments involving changing the electrode potential and modifying the electrode surface with different molecules were carried out. The results indicated that an electrostatic interaction between the charged surface and the charged particles might play a role in the particles' sticking probability. For example, a surface change of a C UME induced by piranha treatment resulted in about a five times higher sticking frequency (Figure 6).

Another important factor affecting the collision behavior is the capping agents on the NP surface. These species are often long alkyl chain species with thiol, amine, or carboxylic acid end groups, dendrimers, or polymers. They affect the catalytic properties of the NP surface[18] and the interaction between the NPs and electrode as well. We carried out ligand replacement on the Pt NPs of citrate ions by long SAMs of alkane thiols and studied the collision behavior (Figure 7a and b). The electrocatalytic activity of Pt NPs for hydrazine oxidation gradually decreased with an increase in the concentration of the SAM (of the same carbon chain length). This was attributed to the gradual blockage of the active sites on the NP surface toward inner sphere reactions. This result demonstrated that a quick screen of the catalytic properties of nanoparticles at the single particle level might be achieved by electrocatalytic amplification.

3. Metal and IrO_x NPs (Nonsticking and Transient (Blip) Response)

3.1. Iridium Oxide (IrO_x)/Pt, Au Electrode/Water (OH^-) Oxidation

In the previous sections, we described single NP collisions, where a stepwise current increase was found when a Pt NP contacted an electrode surface and stuck.[11,16]

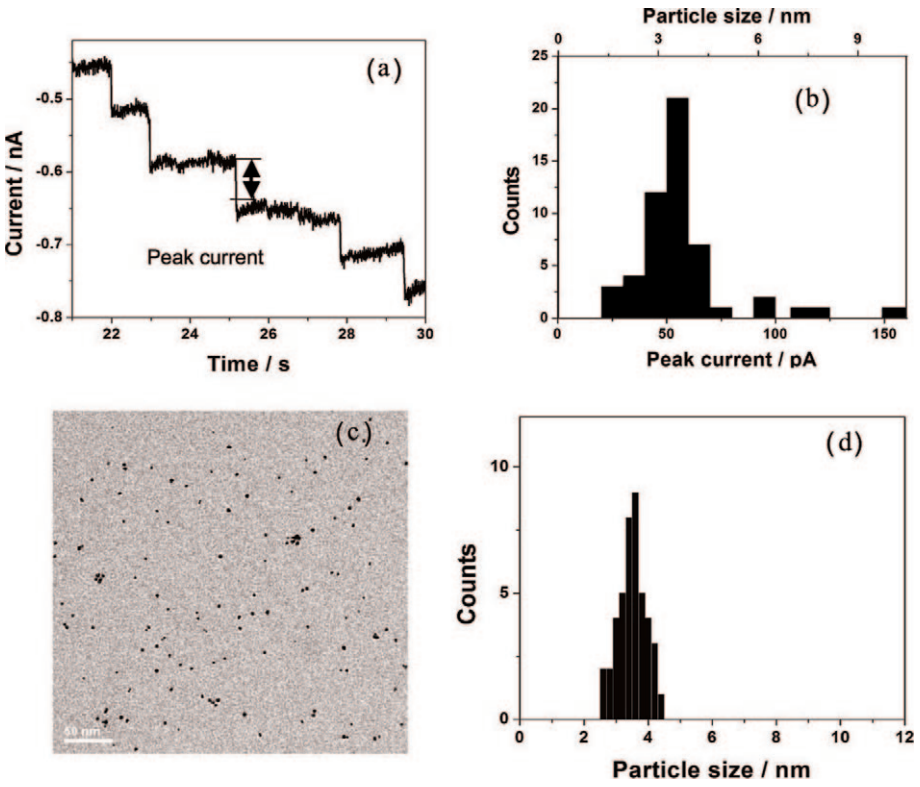

Figure 5. (a) Representative current steps from Figure 4b. (b) Statistical peak current versus peak frequency analyzed for a 200-s interval. (c,d) TEM image and size distribution of the corresponding Pt NPs.

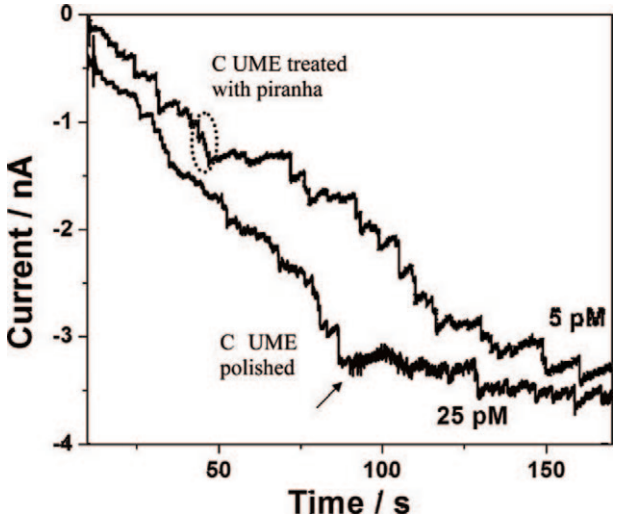

Figure 6. Current transients recorded before and after injection of Pt NPs at a C UME polished and further treated with piranha solution. Electrode potential, 0.5 V vs. NHE; Pt NP size, ~3.6 nm; test electrolyte, 15 mM hydrazine, 50 mM PBS buffer.

Based on the same enhanced current by electrocatalytic redox recycling, we could also detect electrochemically single IrO_x NP collisions at the UME.[19] However, the IrO_x NP collisions were "elastic" rather than "sticking," resulting in a "blip" rather than a "staircase" response. Here one observes current spike transients, with the background current level remaining steady, even after multiple collisions.

IrO_x is a good electrocatalyst for water oxidation.[20] As shown in Figure 8, without IrO_x NPs, water oxidation at a Au UME in an aqueous solution pH 13 is small at an applied potential above 0.7 V (vs. Ag/AgCl). However, it is accelerated in the presence of IrO_x NP (~30 nm diameter). As illustrated in Scheme 1, when the IrO_x NP is far from the electrode surface, the Au electrode itself can't catalyze water oxidation reaction at a bias of 0.8 V (vs. Ag/AgCl). However, when an IrO_x NP approaches the electrode, we can observe an enhanced water oxidation current, which is catalyzed by an IrO_x NP. The electrochemically generated Ir^{VI} state in the NP is proposed to act as a redox catalyst for water oxidation on the electrode surface.[21] When the IrO_x NP leaves the electrode surface, the redox cycling stops. This causes the current spike illustrated in the inset of Scheme 1 and the series of blips shown in Figure 9. When the NP comes within electron transfer distance to the electrode, the current immediately increases and then decays as the particle diffused away. There is probably some stickiness in the electrode interaction, as well as actual multiple collisions with the electrode while the NP is at or near the surface. The current spikes were quite uniform, although there were some

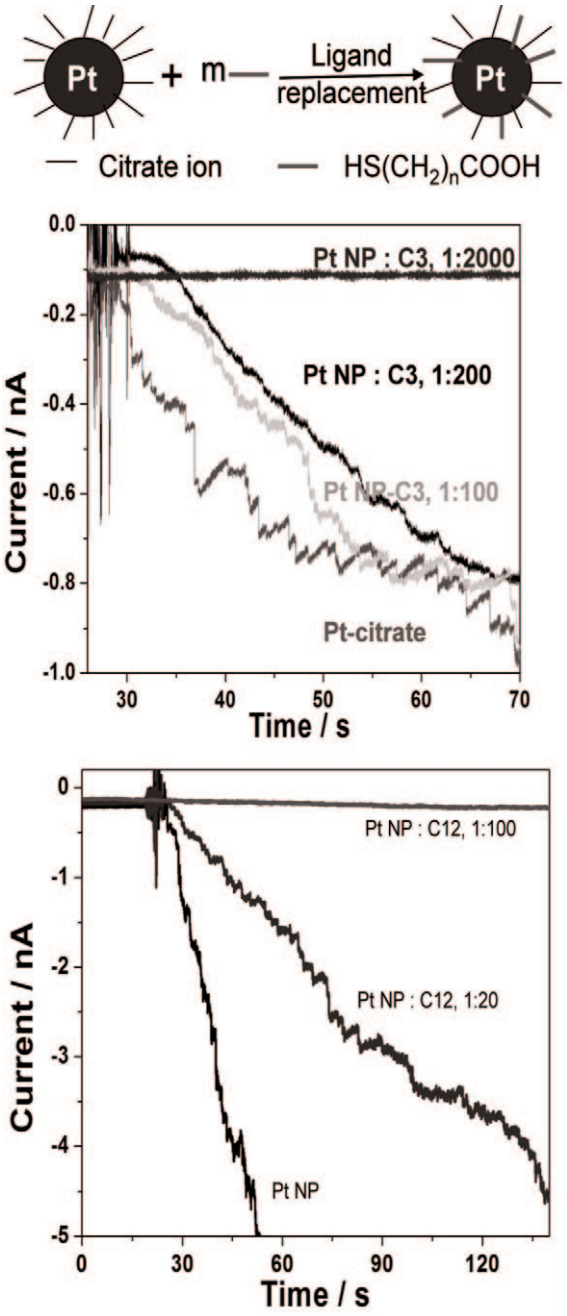

Figure 7. Current transients recorded at Au UMEs before and after injection of Pt NPs capped by a mixture of citrate ions and (a) C3 SAMs and (b) C12 SAMs. Replacement of citrate by SAMs is illustrated at the top of the figure. Au UMEs 10 μm in diameter, electrode potential 0.1 V vs. NHE, particle size ~3.6 nm, particle concentration ~50 pM, electrolyte 12 mM hydrazine + 50 mM PBS buffer, pH ~7.5, C3:3-mercaptopropanoic acid, C12: 12-mercaptododecanoic acid.

differences in shape and height, which probably indicate differences in the size and shape of the particular NP.

Current transients at potentials above 0.7 V vs. Ag/AgCl showed that the height of the current spikes increased with applied potential, while with a bias of 0.7 V

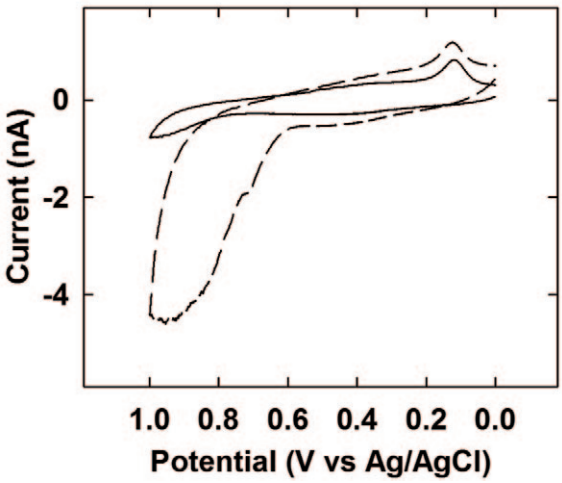

Figure 8. Cyclic voltammograms of water oxidation at Au UME (radius 5 μm) in pH 13 solution (0.1 M NaOH) containing 0 (solid line) or 9.6 pM IrO_x NPs (dashed line). Scan rate is 50 mV/s.

or below, we observed no current transients (data not shown). This is consistent with the voltammogram in Figure 8, which shows the onset of water electrolysis at about 0.62 V (vs. NHE).

The magnitude of the current spike is affected by many variables, such as size and shape of the NP, its residence time on the electrode, concentration, C_p, and diffusion coefficient, D_p, of reactant, applied potential, the rate constants of the reactions, and surface state of an electrode.[22] We could compare the transient to the diffusion-limited current generated by a spherical NP attached to a planar electrode,[22] 23 nA, and the experimentally obtained average current spike, 15 pA. The large difference between calculated and experimentally obtained values suggests that the current is controlled by the residence time of the NP and the rate of OH^- oxidation. The collision frequency increased in proportion to the particle concentration as shown in Figure 10. In this study, the particles do not irreversibly stick and thus do not generate a concentration gradient, so the collision frequency can't be calculated exactly from the steady-state diffusion-controlled flux of particles to the UME surface as is used in Pt NP collision. Rather the frequency of arrival at the electrode surface is given by an approximate equation of the same form

$$n_{p,s} \approx 4\pi D_p C_p a \quad (2)$$

where a is the radius of the UME disk electrode.[23] However, the estimated diffusion arrival frequency is about ten times higher than the experimental value, suggesting that all arrivals at the electrode surface do not result in measureable transients.

The shape and frequency of the current transients are affected not only by the NPs, but also by the material and

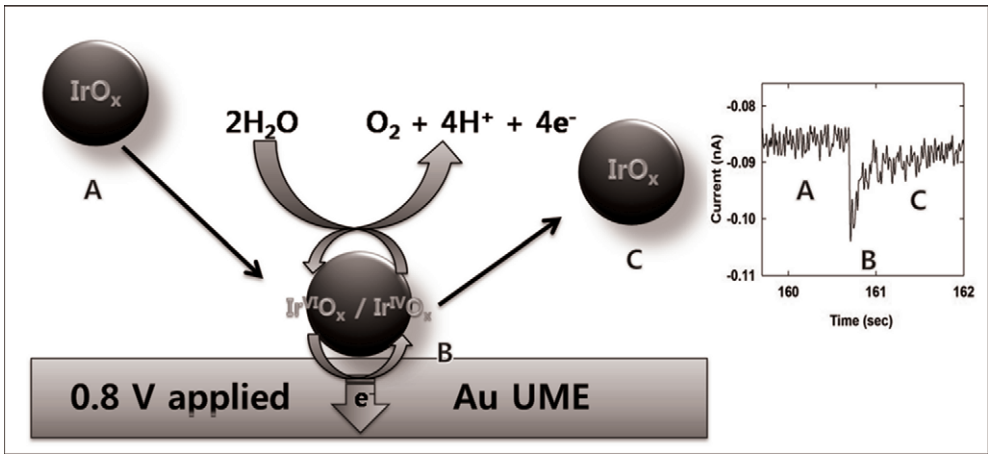

Scheme 1. Schematic illustration of single IrOx NP collision event and the current enhanced by electrocatalytic water oxidation.

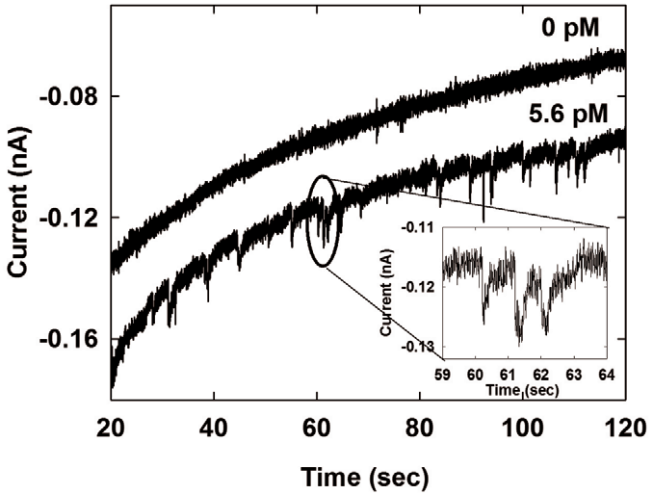

Figure 9. Chronoamperometric curves for single IrO_x NPs (radius, ~30 nm) collisions at the Au UME (radius 5 μm) in pH 13 solution (0.1 M NaOH) without (0 pM) and with (5.6 pM) IrO_x NPs. Applied potential is 0.8 V (vs. Ag/AgCl). Data acquisition time is 10 ms.

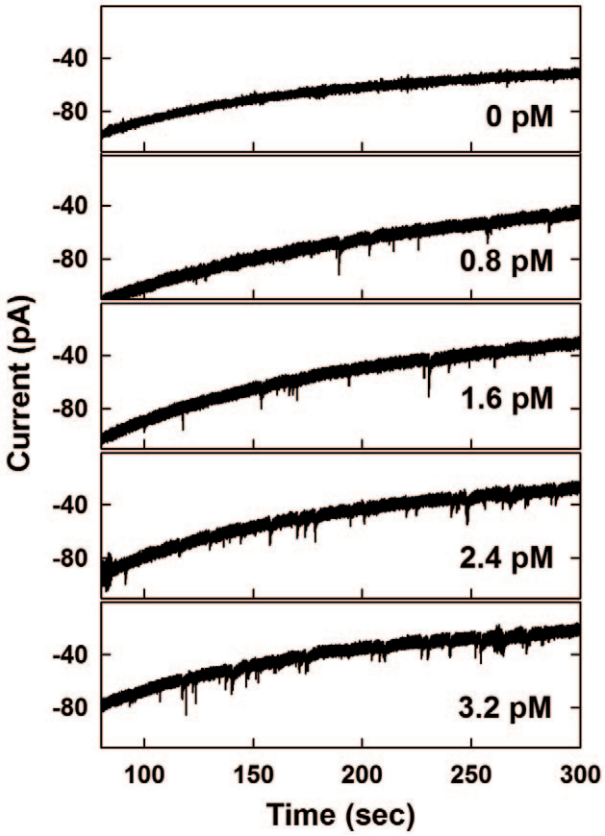

Figure 10. Chronoamperometric curves for single IrO_x NP collisions at the Au UME (radius 5 μm) in pH 13 solution (0.1 M NaOH) containing various concentration of IrO_x NPs from 0 to 3.2 pM. Applied potential is 0.8 V (vs. Ag/AgCl). Data acquisition time is 10 ms.

nature of the surface of the measuring electrode. For example, citrate-stabilized IrO_x NPs do not stick to a Pt or Au electrode during collision and water oxidation,[19] but citrate-stabilized Pt NPs stick to a C or Au electrode during proton reduction or hydrazine oxidation.[19] As for the electrode material, the current transients of IrO_x NP collisions are frequent on bare Au, rare on bare Pt, and not seen on carbon fiber UMEs. Thus, the electrocatalytic redox recycling behavior depends strongly on the electrode material. The current spikes are sensitive to the electrode surface, and we find that the current transient behavior can be modified with different treatments, e.g., by immersing the Pt UME in a 10 mM aqueous $NaBH_4$ solution for 5 min.[19] This electrode-surface-based behavior is still not well understood, but the single NP collision technique can be a useful tool to study such phenomena.

3.2. Au NPs /Pt-PtO_x Electrode/BH_4^- Oxidation[24]

As an example of manipulation of the electrode surface behavior to observe Au NP effects, consider the case of $NaBH_4$ oxidation. This reaction shows different activity on different electrode materials,[25,26] e.g., when studied in

10 mM $NaBH_4$ dissolved in 0.1 M NaOH to suppress hydrolysis. As shown in Figure 11a, the oxidation of $NaBH_4$ starts at negative potentials at both Au and Pt UMEs. Pt shows better catalytic activity than Au (the onset potential for oxidation is more negative), so one would think that a Pt electrode couldn't be used as substrate to observe Au NP effects. However, one can manipulate the surfaces of Pt and Au, for example by forming oxide, which is known to inhibit inner sphere reactions because of loss of active sites for catalytic reaction. Thus, cyclic voltammetry of $NaBH_4$ oxidation shows markedly decreased activity when the potential is scanned positively. In scanning in the negative direction from positive potentials, gold oxide is reduced earlier than Pt oxide and retains all active sites before Pt oxide gets reduced to Pt (Figure 11b). This creates a potential window to observe Au NP collisions on a Pt/PtO_x UME.

A two-step approach was used: (step 1) a potential step to 0.9 V (vs. Ag/AgCl) was applied to grow oxide on the Pt surface, and (step 2) the potential was then stepped 0 V (vs. Ag/AgCl) such that the oxide is maintained under these conditions, even in the presence of BH_4^-, and Au NP collisions can be observed for BH_4^- oxidation, as shown in Figure 11c. The oxidation at 0.9 V caused the current for BH_4^- oxidation to be very small on the Pt UME. However, Au still showed good catalytic activity for BH_4^- oxidation at 0 V (vs. Ag/AgCl). The current–time curve after injection of Au NPs (made by the citrate reduction method)[27] on a pre-oxidized Pt electrode is shown in Figure 12a. The average particle size was ~14 ± 0.5 nm. For each collision, the current increased quickly and then decreased back to the background level, resulting, as in the previous IrO_x case, in a series of blips. The amplitude of each current peak depends on the particle size, residence time, rate constants, and the interaction between the NPs and the electrode. These combined effects make the number of charges transferred in each electrode interaction different, which accounts for the different amplitudes of the current peaks. A single peak is shown in Figure 12b, and the total charge transferred (through integrating the area under this peak) is about 2×10^{-11} C.

The amplitude of current peak is also dependent on the holding potential (e.g., 0 V (vs Ag/AgCl) in Figure 12). When this potential was made more positive, the amplitude of the peaks decreased; above 0.4 V (vs. Ag/AgCl), very few or no peaks were observed. This can be explained by the behavior of the Au NPs. At these potentials, when the Au NPs contact the electrode they become oxidized, and the oxide layer on the surface blocks active

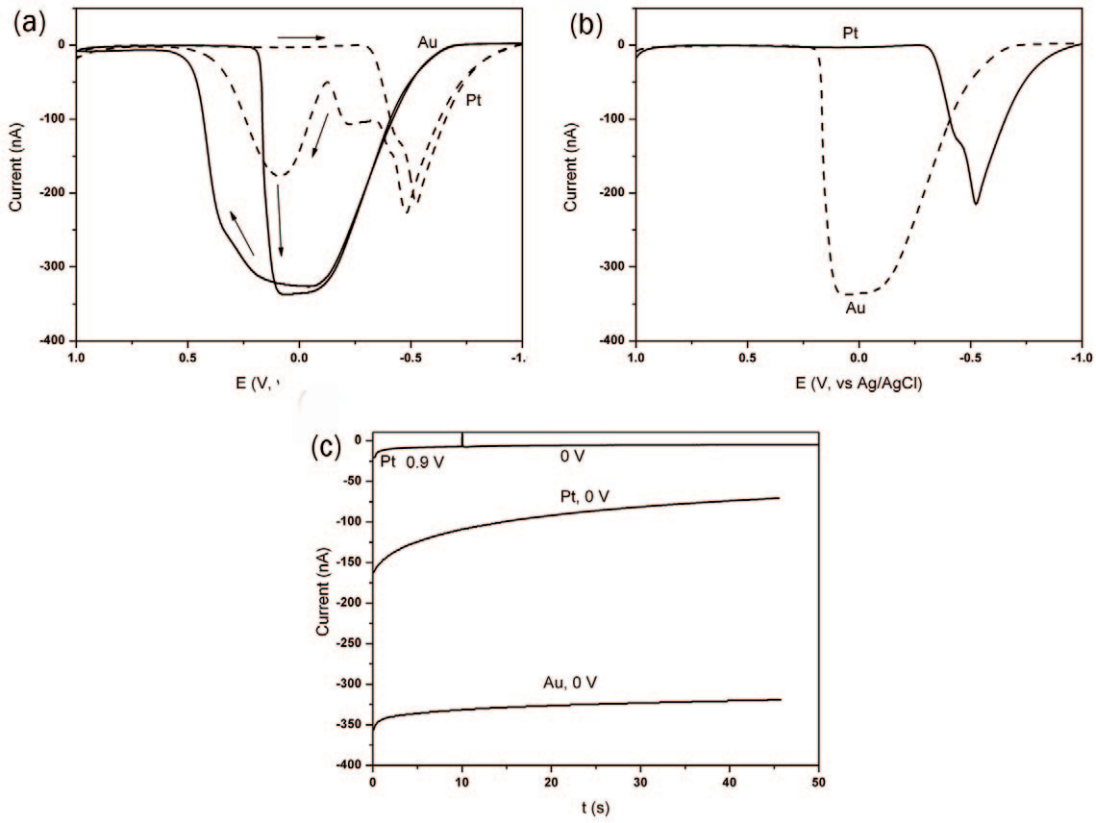

Figure 11. (a) Cyclic voltammetry of Au and Pt UME. (b) Negative scan in panel (a). (c) Potential step measurement on Au and Pt UME, value and sequence of applied potentials are shown in the panel. UME diameter, 10 μm; sweep rate, 100 mV/s; electrolyte, 10 mM $NaBH_4$, 0.1 M NaOH solution.

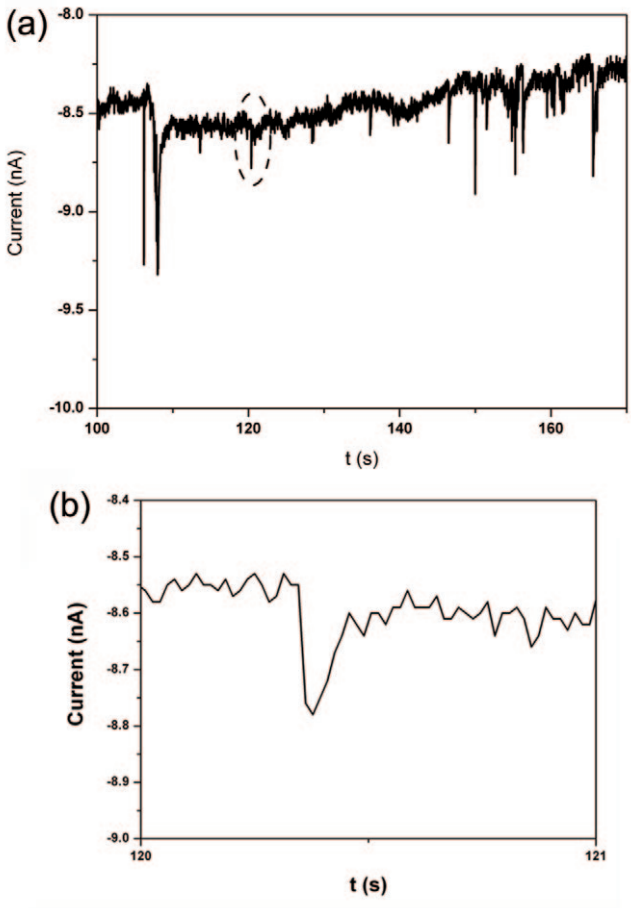

Figure 12. (a) Current time curve at a pre-oxidized Pt electrode (10 μm) in 10 mM $NaBH_4$, 0.1 M NaOH solution. (b) Zoom of (a) showing a single collision peak. Au NP concentration, 24 pM; potential, 0 V (vs. Ag/AgCl).

sites for $NaBH_4$ oxidation. This work demonstrates that an active electrode (Pt) can be conveniently turned into an inert electrode by oxide film formation (Pt/PtO_x) or other suitable surface modification.

4. Summary and Outlook

Collisions of single nanoparticles with an electrode can be observed and can potentially provide new insight into electrochemical reactions. A firm theoretical understanding of the response will require stochastic models and a better understanding of factors like the NP sticking probability, the sticking time, electron transfer probabilities, and deactivation processes. In addition to the fundamental scientific aspects of the work, such studies may find applications in observing single particle electrocatalysis, where a better characterization of the structural nature of the catalyst can be determined. It may also find application in electroanalysis, where the NPs are used as labels, e.g., with biomolecules, to obtain very high sensitivities. Other applications, like determination of particle size distributions in solution and using the NPs as probes of surface layer permeability, can also be considered.

Acknowledgments

We thank the National Science Foundation (CHE 0808927) and the Texas Higher Education Coordinating Board ARP (003658-0156-2007) for support of this research.

References

[1] See, e.g., W. E. Moerner, L. Kador, *Phys. Rev. Lett.* **1989**, *62*, 2535–2538.
[2] M. Orrit, J. Bernard, *Phys. Rev. Lett.* **1990**, *65*, 2716–2719.
[3] R. E. Palacios, F.-R. F. Fan, A. J. Bard, P. F. Barbara, *J. Am. Chem. Soc.* **2006**, *128*, 9028–9029.
[4] R. E. Palacios, F.-R. F. Fan, J. K. Grey, J. Suk, A. J. Bard, P. F. Barbara, *Nature Mater.* **2007**, *6*, 680–685.
[5] F.-R. F. Fan, A. J. Bard, *Science* **1995**, *267*, 871–874.
[6] F.-R. F. Fan, J. Kwak, A. J. Bard, *J. Am. Chem. Soc.* **1996**, *118*, 9669–9675.
[7] F.-R. F. Fan, A. J. Bard, *Acc. Chem. Res.* **1996**, *29*, 572–578.
[8] P. Sun, M. V. Mirkin, *J. Am. Chem. Soc.* **2008**, *130*, 8241–8250.
[9] R. J. White, H. S. White, *Anal. Chem.* **2005**, *77*, 215 A–220 A.
[10] P. A. Bobbert, M. M. Wind, J. Vlieger, *Physica A* **1987**, *141*, 58–72.
[11] X. Xiao, A. J. Bard, *J. Am. Chem. Soc.* **2007**, *129*, 9610–9612.
[12] J. F. Zhou, Y. B. Zu, A. J. Bard, *J. Electroanal. Chem.* **2000**, *491*, 22–29.
[13] J. Yang, J. Y. Lee, H. P. Too, *Anal. Chim. Acta* **2006**, *571*, 206–210.
[14] D. Pletcher in *Microelectrodes: Theory and Application* (Eds.: M. I. Montenegro, M. A. Qjueiros, J. L. Daschbach), Kluwer, Dordrecht, **1991**, p. 472.
[15] X. Y. Xiao, B. Q. Xu, N. J. Tao, *Nano Lett.* **2004**, *4*, 267–271.
[16] X. Xiao, F.-R. F. Fan, J. Zhou, A. J. Bard, *J. Am. Chem. Soc.* **2008**, *130*, 16669–16677.
[17] X. Xiao, S. Pan, J. S. Jang, F.-R. F. Fan, A. J. Bard, *J. Phys. Chem. C* **2009**, *113*, 14978–14982.
[18] D. K. Park, S. J. Lee, J.-H. Lee, M. Y. Choi, S. W. Han, *Chem. Phys. Lett.* **2010**, *484*, 254–257.
[19] S. J. Kwon, F.-R. F. Fan, A. J. Bard, ASAP.
[20] a) P. G. Hoertz, Y.-I. Kim, W. J. Youngblood, T. E. Mallouk, *J. Phys. Chem. B* **2007**, *111*, 6845–6856; b) T. Nakagawa, C. A. Beasley, R. W. Murray, *J. Phys. Chem. C* **2009**, *113*, 12958–12961; c) M. Yagi, E. Tomita, S. Sakita, T. Kuwabara, K. Nagai, *J. Phys. Chem. B* **2005**, *109*, 21489–21491.
[21] T. Nakagawa, N. S. Bjorge, R. W. Murray, *J. Am. Chem. Soc.* **2009**, *131*, 15578–15579.
[22] A. J. Bard, L. R. Faulkner, *Electrochemical Methods, Fundamentals and Applications*, 2nd ed.; Wiley, New York, **2001**.
[23] The collision frequency is caused by Brownian motion of the particle and will be discussed in another publication in preparation.

[24] H. Zhou, F.-R. F. Fan, A. J. Bard, *J. Phys. Chem. Lett.* **2010**, *1*, 2671–2674.
[25] H. Celikkan, M. Sahin, M. L. Aksu, T. N. Veziroglu, *Int. J. Hydrogen Energy* **2007**, *32*, 588–593.
[26] B. M. Concha, M. Chatenet, *Electrochim. Acta* **2009**, *54*, 6119–6129.
[27] L. Qian, Q. Gao, Y. Song, Z. Li, X. Yang, *Sens. Actuators, B* **2005**, *107*, 303–310.

Received: April 15, 2010
Accepted: August 24, 2010
Published online: September 17, 2010